EPR of Gd^{3+}-doped single crystals of $LiYF_4$ and $LiYbF_4$: Gd^{3+}-Yb^{3+} exchange constant

Sushil K. Misra and Mojtaba Kahrizi
Department of Physics, Concordia University, 1455 de Maisonneuve Boulevard West, Montreal, Quebec, Canada H3G 1M8

P. Mikolajczak and L. Misiak
Department of Experimental Physics, Marie Curie-Sklodowska University, 20-031 Lublin, Poland

(Received 28 January 1985)

X-band EPR measurements on Gd^{3+}-doped single crystals of $LiYF_4$ and $LiYbF_4$ are performed at room and low temperatures. The spin-Hamiltonian parameters are estimated with the use of a rigorous least-squares-fitting computer technique. The behavior of the linewidths and the spin-Hamiltonian parameters, as a function of temperature, are studied. The total exchange interaction of Gd^{3+} with its nearest and next-nearest paramagnetic Yb^{3+} neighbors in the $LiYbF_4$ host crystal is estimated with the use of the *g*-value shift of Gd^{3+} in the paramagnetic lattice of $LiYbF_4$, from that in the isostructural diamagnetic lattice of $LiYF_4$.

I. INTRODUCTION

$LiYF_4$ is an interesting host material for lasers.[1] EPR of Gd^{3+}-doped scheelite compounds, which are isostructural to $LiYF_4$, has been extensively studied.[2] EPR measurements on Gd^{3+}-doped single crystals of $LiYF_4$ have been reported by Vaills and Buzare.[3] They gave a detailed analysis of the EPR spectra of Gd^{3+} in this crystal at room temperature only. They provided an explanation of the observed parameters on the basis of electrostatic[4] and superposition[5] models. The purpose of the present paper is to report detailed *X*-band EPR measurements on Gd^{3+}-doped $LiYF_4$ and $LiYbF_4$ single crystals at various temperatures. The measurements on the $LiYbF_4$ host are the first ever to be reported. As for the host $LiYF_4$, the measurements will be extended to liquid-helium temperature. The emphasis here will be to estimate precisely the spin-Hamiltonian parameters for both the hosts at various temperatures. To this end, a rigorous computer technique based on least-squares-fitting criterion using numerical evaluation of eigenvalues and eigenvectors, simultaneously fitting all resonant line positions obtained for several orientations of the external magnetic field,[6] is used. Last, but not of least importance, the Gd^{3+}-Yb^{3+} exchange interaction in the $LiYbF_4$ host will be determined from the shift of the Gd^{3+} *g* value in the paramagnetic $LiYbF_4$ host from that in the isostructural diamagnetic host $LiYF_4$. Similar determinations of Mn^{2+}-Ni^{2+} exchange interaction have been previously reported.[7-9]

II. SAMPLE PREPARATION AND CRYSTAL STRUCTURE

A modified Bridgman-Stockbarger method was used to grow $LiYF_4$ and $LiYbF_4$ single crystals doped with 0.1 mol% of GdF_3. The single crystals were grown in an induction furnace, using a frequency of 460 kHz. A quartz tube was installed inside the coil, locked by a cover with the rubber seal. Inside the tube was placed the graphite shield along with the thermocouple. The pot was connected to a small motor by a rod through the gear system (Fig. 1), with which the graphite melting pot could be shifted. The graphite melting pot was provided with a sharp conelike bottom and a cover to lock its upper inlet in order to obtain single crystals.

Rare-earth (Y, Yb) fluorides of 99.9% purity and lithium fluoride of 99.5% purity were obtained from Alfa-Ventron (USA). Further purification of LiF was accomplished by

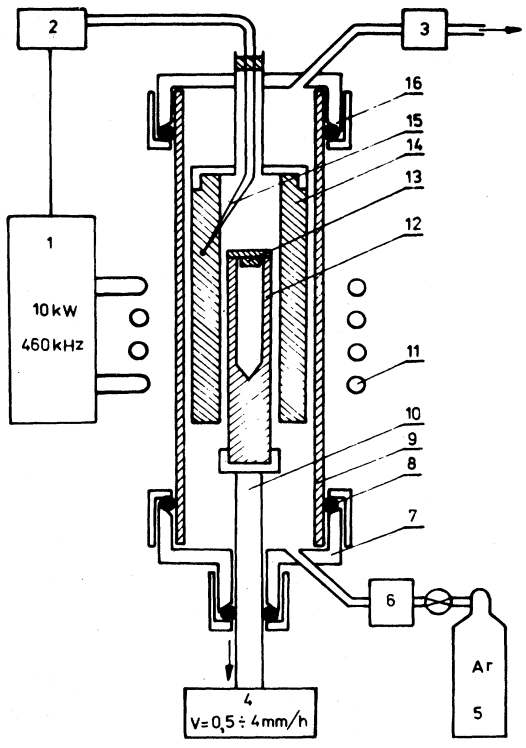

FIG. 1. Block diagram of the apparatus used for the growth of Gd^{3+}-doped $LiYF_4$ and $LiYbF_4$ single crystals. The details are as follows: (1) generator, (2) temperature stabilizer, (3) recorder of the gas flow, (4) motor, (5) argon container, (6) absorber of the water vapor, (7) bottom cover, (8) rubber seal, (9) quartz tube, (10) metal rod, (11) induction coil, (12) graphite melting pot, (13) graphite lock, (14) graphite shield, (15) thermocouple, (16) upper cover (air cooled).

growing single crystals out of the polycrystalline powder. The rare-earth fluorides were first dried for 3 h under constant flow of argon at temperatures of 150 and 500 °C. They were then kept for 3–5 h at temperatures higher than their respective melting points. To fluorize and purify these substances PbF_2 was used in the amount of about 1% of the total weight.

The purified rare-earth fluorides and LiF single crystals were used to prepare the mixture for synthesis and crystal growth of Gd^{3+}-doped $LiYF_4$ and $LiYbF_4$. The composition of the mixture was chosen to be that described in Ref. 10. The pressure of the LiF vapors is higher than that of the rare-earth fluorides. Thus an excess of LiF anywhere from 2 to 4 mol% was used. The synthesis and homogenization of the mixture was performed for 2–4 h in the temperature range 1000–1100 °C. The crystals were grown under constant flow of argon gas, at the rate 1 liter/min. The temperature was maintained to be at least 50 °C higher than the melting point of the particular compound (819 °C for $LiYF_4$ and 850 °C for $LiYbF_4$). A temperature gradient of 100 °C/cm was used, while the drop rate of the melting pot was 4.5 mm/h. The temperature of the graphite shield was stabilized within ±2 °C. The measured lattice constants of the grown sample calculated from the observed x-ray diffraction correspond very closely to the data available in the literature.[10]

The crystal structure of $LiYF_4$ and $LiYbF_4$ have been reported in Refs. 11 and 12. Both have $CaWO_4$-type (scheelite) structure, crystallizing in tetragonal structure with the space-group symmetry $I4_1/a$. The unit cell of $LiYF_4$ has the dimensions $a = 5.175 \pm 0.005$ Å and $c = 10.74 \pm 0.01$ Å, while that of $LiYbF_4$ has the dimensions $a = 5.132 \pm 0.005$ Å and $c = 10.59 \pm 0.01$ Å. Each rare-earth ion is surrounded by eight nearest-neighbor fluorines, four of which are at a distance $R_1 = 2.246$ Å, while the remaining four are at a distance $R_2 = 2.293$ Å.

III. EXPERIMENT

The EPR spectra were recorded using a homodyne X-band spectrometer, equipped with 100 kHz field modulation.[13] A Varian magnet with 12-in. pole pieces was used to provide the magnetic field, which was controlled by a Fieldial-Mark II power supply. The magnetic field was measured using a Bruker model B-NM 20 nuclear-magnetic-resonance oscillator; a calibration curve was used to estimate the actual magnetic field at the location of the sample inside the cavity.

The EPR spectra of Gd^{3+}-doped $LiYF_4$ were recorded at room, liquid-nitrogen, and liquid-helium temperatures in the ZX and XY planes (X, Y, Z axes are defined in Sec. IV). At room temperature, seven well-resolved lines were observed in the range 400–9600 G, for the magnetic field orientation along the Z axis. Besides the allowed lines, some forbidden lines were also observed at lower magnetic field values; the number of these lines increased as the magnetic field direction moved away from the Z axis, in accordance with the description given in Ref. 3. Figure 2 exhibits the angular variation of EPR spectra of Gd^{3+}-doped $LiYF_4$ at room temperature, in the ZX plane.

As the temperature was lowered from room to liquid helium, the general features of the spectra remained the same; however, the overall splitting of the spectra increased and the intensities of lines at lower magnetic fields, increased relative to those at higher fields. The latter observation implies that the sign of the zero-field splitting parameter b_2^0 is negative.[14]

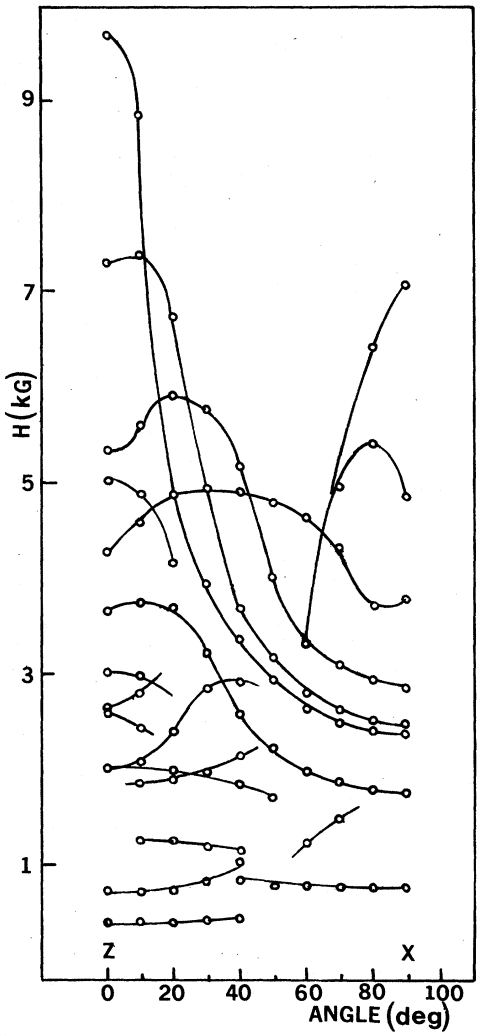

FIG. 2. Angular variation of room-temperature X-band spectra for Gd^{3+}-doped $LiYF_4$ host in the ZX plane. The circles represent the experimental resonant-line positions, while the solid lines are smooth curves that connect data points for the same transition.

As for Gd^{3+}-doped $LiYbF_4$, the EPR spectra in this crystal at room temperature had the same features as those for Gd^{3+}-doped $LiYF_4$, except the linewidths were larger (due to the dipole-dipole interaction between Gd^{3+} and the paramagnetic host ions Yb^{3+}). As the temperature was lowered below room temperature, the lines started to broaden rapidly; below 270 K the lines completely disappeared (for more details see Sec. V).

IV. SPIN HAMILTONIAN AND EVALUATION OF PARAMETERS

The following spin Hamiltonian,[14] corresponding to tetragonal symmetry, was used to fit EPR data:

$$\mathcal{H} = \mu_B \mathbf{H} \cdot \tilde{g} \cdot \mathbf{S} + \tfrac{1}{3} b_2^0 O_2^0 + \tfrac{1}{60}(b_4^0 O_4^0 + b_4^4 O_4^4) + \tfrac{1}{1260}(b_6^0 O_6^0 + b_6^4 O_6^4) \quad . \tag{1}$$

TABLE I. Values of spin-Hamiltonian-parameters for the Gd^{3+}-doped $LiYF_4$ and $LiYbF_4$ hosts (0.1 mol% each) at various temperatures. g is dimensionless, while b_l^m are expressed in GHz. The indicated errors are as calculated by the use of a statistical method (Ref. 16). The parameters at room temperature (RT), as reported in Ref. 3, have also been included for comparison.

	$LiYF_4$				$LiYbF_4$
Temperature	295 K	85 K	5 K	RT (Ref. 3)	295 K
g_{zz}	1.9890 ±0.0010	1.9813 ±0.0016	1.9804 ±0.0016	1.9837 ±0.0005	1.9864 ±0.0076
g_{xx}	1.9871 ±0.0010	1.9828 ±0.0016	1.9837 ±0.0016	1.9825 ±0.0005	1.9870 ±0.0076
b_2^0	−2.4837 ±0.0015	−2.5141 ±0.0017	−2.5183 ±0.0017	±2.4810 ±0.0150	−2.4892 ±0.0170
b_4^0	−0.0671 ±0.0004	−0.0667 ±0.0006	−0.0667 ±0.0006	±0.0570 ±0.0030	−0.0508 ±0.0017
b_4^4	0.2778 ±0.0030	0.4241 ±0.0040	0.4366 ±0.0040	∓0.3030 ±0.0150	0.4144 ±0.0300
b_6^0	−0.0079 ±0.0004	−0.0103 ±0.0008	−0.0145 ±0.0008	0.0000 ±0.0060	−0.0102 ±0.0020
b_6^4	0.0216 ±0.0060	0.0611 ±0.0100	0.0939 ±0.0100	±0.0165 ±0.0150	0.1788 ±0.0400

In Eq. (1) H is the external magnetic field, μ_B is the Bohr magneton, S ($=\frac{7}{2}$) is the electron spin of Gd^{3+}, b_l^m are the spin-Hamiltonian parameters, and O_l^m are the spin operators as given by Abragam and Bleaney.[14] The X,Y,Z axes are chosen so as to coincide with the principal axes of the b_2^m tensor; thus, the overall splitting of the spectra is maximum along the Z axis and minimum along the Y axis.[15]

The spin-Hamiltonian parameters were evaluated using a least-squares-fitting procedure,[6] fitting simultaneously all clearly resolved line positions obtained in the ZX plane. The fitting gave the correct relative signs of the parameters. The absolute signs of the parameters were obtained by determining the absolute sign of b_2^0 using the observed relative intensities of lines at liquid-helium temperature. (The absolute sign of b_2^0 was found to be negative for the $LiYF_4$ host, since the intensity of the highest-field line relative to that of the lowest-field line for the magnetic field orientation along the Z axis reduced by a factor of 7 in going from room to liquid-helium temperature. The sign of b_2^0 for Gd^{3+}-doped $LiYbF_4$ was also assumed to be negative since it could not be determined due to the disappearance of the lines below 270 K.) The errors were calculated by the use of a statistical method.[16] The spin-Hamiltonian parameters for Gd^{3+}-doped $LiYF_4$ and $LiYbF_4$ are listed in Table I, wherein the values reported by other authors[3] are also given for comparison.

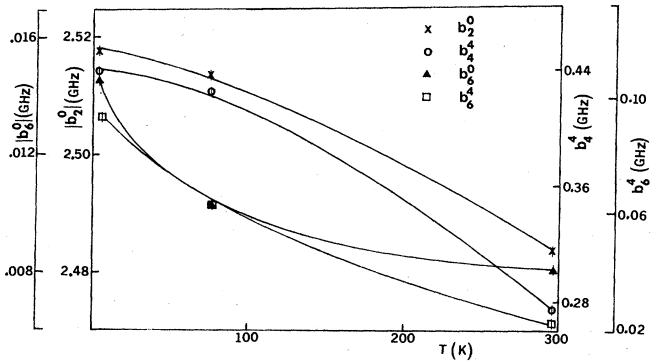

FIG. 3. Variation of the spin-Hamiltonian parameters $|b_2^0|$, b_4^4, $|b_6^0|$, and b_6^4 for Gd^{3+}-doped $LiYF_4$ host as a function of temperature. The scale for each parameter is separately indicated.

The absolute values of all the spin-Hamiltonian parameters for the $LiYF_4$ host increase with decreasing temperature, except for b_4^0, which remains invariant within experimental error. Figure 3 displays the temperature variation of the parameters. It is seen that these parameters do not display a linear variation with temperature, and it would be interesting to look for mechanisms which predict such a nonlinear variation of parameters with temperature.

V. LINEWIDTH

No magnetic field dependence of linewidths was observed for either samples at any temperature.

The EPR linewidths for Gd^{3+} in the (diamagnetic) lattice of $LiYF_4$ were about 40 G for the various lines at room temperature, which increased to about 49 G as the temperature was lowered to liquid-helium temperature. For the paramagnetic lattice of $LiYbF_4$, the linewidths were larger, about 105 G at room temperature, due to the interaction between Gd^{3+} and the paramagnetic Yb^{3+} ions. As the temperature was lowered from room temperature, most of the lines disappeared, and only one line in the low magnetic-field region could be observed down to 270 K, below which no lines were observed.

VI. g-VALUE SHIFT AND EXCHANGE INTERACTION

Owing to the interaction between Gd^{3+} and Yb^{3+} in the paramagnetic lattice of $LiYbF_4$ the g value for Gd^{3+} in this sample will be shifted from that in the isostructural diamagnetic lattice of $LiYF_4$.

Assuming that the interaction of the Gd^{3+} with Yb^{3+} involves both the magnetic dipole and exchange interaction, the g-value shift was calculated by Birgeneau, Hutchings, and Wolf[17] to be as follows, considering only the nearest neighbor (NN) and next-nearest neighbor (NNN):

$$\delta g_z = \left(\frac{-8}{\Delta}\right)[4J_{NN} - 8\alpha_{NN} + 4J_{NNN} + 4\alpha_{NNN}(1-3\cos^2\theta)] , \tag{2}$$

$$\delta g_x = \left(\frac{-8}{\Delta}\right)[4J_{NN} + 4\alpha_{NN} + 4J_{NNN} - 2\alpha_{NNN}(1-3\cos^2\theta)] , \tag{3}$$

where Δ is the energy separation between the ground and

the first excited states of the host Yb^{3+} ion, the J's are the exchange integrals, the α's represent the strength of the magnetic dipole-dipole interactions, and θ is the angle that the magnetic field makes with the bond between Gd^{3+} and the next-nearest neighbors. The α's are given by $\alpha_i = g\mu^2/r_i^3$, where g and μ are the g factor and the magnetic moment, respectively, of the host ion Yb^{3+}, and r_i is the distance between Gd^{3+} and the ith Yb^{3+}.

The isotropic part of the single-ion g-value shift is independent of the magnetic dipole interaction since

$$(\delta g_z + 2\,\delta g_x) = (g_z + 2g_x)_{\text{para}} - (g_z + 2g_x)_{\text{dia}} = -\left[\frac{96}{\Delta}\right](J_{\text{NN}} + J_{\text{NNN}}) \ , \quad (4)$$

while the anisotropic part is independent of the exchange interaction since

$$(\delta g_z - \delta g_x) = (g_z - g_x)_{\text{para}} - (g_z - g_x)_{\text{dia}} = \frac{48}{\Delta}[2\alpha_{\text{NN}} - \alpha_{\text{NNN}}(1 - 3\cos^2\theta)] \ . \quad (5)$$

Using Eq. (4) and $\Delta = 29.49 \times 10^4$ GHz,[18] the total exchange interaction between Gd^{3+} and its nearest and next-nearest paramagnetic Yb^{3+} neighbor in $LiYbF_4$ ($J_{\text{NN}} + J_{\text{NNN}}$) was estimated to be 8.601 GHz.

The g_{zz} and g_{xx} values are smaller than those usually found for Gd^{3+} (1.992), suggesting either a large mixing of the excited states with the ground state, or a large covalency effect, or a configuration-mixing effect.[3]

ACKNOWLEDGMENTS

The authors are grateful to the Natural Sciences and Engineering Research Council of Canada Grant No. A4485 for financial support, to Professor G. C. Upreti for a critical reading of the manuscript, and to Concordia University Computer Center for providing their facilities to analyze the data.

[1] D. LeGoff, A. Beltinger, and A. Labadens, Opt. Commun. **26**, 1 (1978).
[2] S. Wishwamitar and S. P. Puri, J. Chem. Phys. **61**, 3270 (1974).
[3] Y. Vaills and J. Y. Buzare, Solid State Commun. **45**, 1093 (1983).
[4] E. J. Bijvink, H. W. Den Hartog, and J. Andriessen, Phys. Rev. B **16**, 1008 (1977).
[5] D. J. Newman and W. Urban, Adv. Phys. **24**, 793 (1975).
[6] S. K. Misra, J. Magn. Reson. **23**, 403 (1976).
[7] S. K. Misra and M. Kahrizi, Phys. Rev. B **28**, 5300 (1983).
[8] S. K. Misra and M. Kahrizi, Phys. Rev. B **30**, 2920 (1984).
[9] S. K. Misra and M. Kahrizi, Phys. Rev. B **30**, 5352 (1984).
[10] *Flouride, Flouride Oxide, and the Related Alkali Double Salts,* edited by H. Berman, Gmelin Handbuck der Anorganischen Chemie Saltenerdelemente, Teil C, Vol. 39 (Springer-Verlag, Berlin, 1976), pp. 270–295.
[11] R. E. Thoma, C. F. Weaver, H. A. Friedman, H. Insley, L. A. Harris, and H. A. Yakel, J. Phys. Chem. **65**, 1096 (1961).
[12] C. Keller and H. Schmutz, J. Inorg. Nucl. Chem. **27**, 900 (1965).
[13] S. K. Misra and M. Jalochowski, Physica B **112**, 83 (1982).
[14] A. Abragam and B. Bleaney, *Electron Paramagnetic Resonance of Transition Ions* (Clarendon, Oxford, 1970).
[15] M. Weger and W. Low, Phys. Rev. **111**, 1526 (1958).
[16] S. K. Misra and S. Subramanian, J. Phys. C **15**, 7199 (1982).
[17] R. J. Birgeneau, M. T. Hutchings, and W. P. Wolf, Phys. Rev. **179**, 275 (1969).
[18] K. A. Gschneidner Jr. and L. R. Eyring, *Handbook on the Physics and Chemistry of Rare-Earths* (North-Holland, Amsterdam, 1979), Vol. 2, p. 478.